

Intrinsic anisotropy of thermal conductance in graphene nanoribbons

Yong Xu, Xiaobin Chen, Bing-Lin Gu, and Wenhui Duan*

Center for Advanced Study and Department of Physics, Tsinghua University, Beijing 100084, China

Thermal conductance of graphene nanoribbons (GNRs) with the width varying from 0.5 to 35 nm is systematically investigated using nonequilibrium Green's function method. Anisotropic thermal conductance is observed with the room temperature thermal conductance of zigzag GNRs up to $\sim 30\%$ larger than that of armchair GNRs. At room temperature, the anisotropy is found to disappear until the width is larger than 100 nm. This intrinsic anisotropy originates from different boundary conditions at ribbon edges, and can be used to tune thermal conductance, which has important implications for the applications of GNRs in nanoelectronics and thermoelectricity.

Graphene nanoribbon (GNR) is believed to be a promising candidate for future nanoelectronic and spintronic devices.^{1,2,3,4} In comparison with intensive research on the electronic transport, the study of the thermal transport in GNRs is not satisfactory until now, despite its importance for nanoelectronics. At present the chip-level power density in integrated circuit is on the order of 100 W/cm^2 , similar to that of nuclear reactor. Increasing circuit density further would induce the exponential increase of power density, so thermal management on individual nanoscale devices becomes vital to ensure stable operation of integrated circuit.⁵ This indicates a full understanding of thermal transport property of GNRs is critical for developing any practical graphene-based devices.

It was previously demonstrated that basic device building blocks can be constructed from GNRs with different widths and edge shapes, which dominates their electronic properties.³ For the evaluation of the overall performance of GNR devices, it is highly important to explore thermal transport characteristics of GNRs with different edge shapes and widths. In fact, a recent work found anisotropic thermal conductance in silicon nanowires (SiNWs): $\langle 110 \rangle$ SiNW exhibits a room temperature thermal conductance 50% and 75% larger than $\langle 100 \rangle$ and $\langle 111 \rangle$ SiNWs.⁶ In contrast, systematical investigation on whether GNRs with different edge shapes give anisotropic thermal conductance is still lacking, despite recent progress in the calculations of thermal conductances of GNRs.^{7,8} A classical molecular dynamics simulation studied thermal conductance for the 1.5 nm wide GNRs with different edges,⁹ but the thermal conductance obtained obviously exceeds the upper ballistic bounds.^{10,11}

In this work, we systematically investigate thermal conductance of GNRs with different widths and edge shapes, and find that thermal conductance of GNRs is primarily proportional to the ribbon width except for GNRs narrower than 2 nm, and more interestingly, exhibits strong anisotropy. Typically, thermal conductance of zigzag GNRs (ZGNRs) are 20% \sim 30% larger than that of armchair GNRs (AGNRs) at room temperature as the ribbon width ranges from 0.5 to 2 nm. Such intrinsic anisotropy decreases with increasing width, but is still

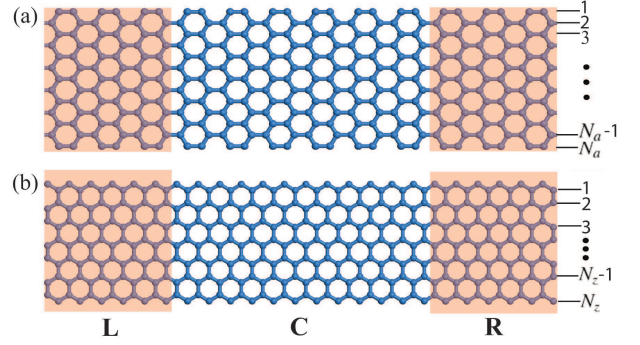


FIG. 1: Schematic illustration of two-probe transport system, where the center transport region (C) is connected to left (L) and right (R) semi-infinite thermal leads. (a) N_a -AGNR, (b) N_z -ZGNR.

larger than 10% even when the width is as large as 35 nm, and thus may have significant effect on the performance of the GNR devices.

Nonequilibrium Green's function (NEGF) method is used to study thermal conductance of GNRs. This method is powerful to treat many body problems when interactions are weak, and can exactly deal with ballistic thermal transport, which gives the maximum thermal conductance of a material.^{12,13,14,15} Since the phonon mean free path is very long in graphene ($\sim 775 \text{ nm}$ at room temperature)¹⁶, the thermal transport is nearly ballistic in pristine GNRs, and thus ballistic thermal conductance is studied in this work. First of all, the second-generation reactive empirical bond order (REBOII) potential,¹⁷ which was proved to give phonon modes of GNRs compatible with density functional theory calculations,¹⁸ is employed to calculate force constants. Then, Green's function and the transmission function $\Xi(\omega)$ of phonon can be calculated for the two-probe transport system (shown in Fig. 1), and finally thermal conductance σ is obtained by Landauer formula.¹⁵ Since GNRs with larger width (W) will have more phonon transport channels and thus larger thermal conductance, the scaled thermal conductance, defined as thermal conductance per unit area (σ/S), is introduced to describe thermal transport properties for materials with different widths. Herein, the cross sectional area S is defined to be $S = W\delta$, where $\delta = 0.335 \text{ nm}$ is chosen as the layer separation in graphite. Following the conventional notation, N_a -AGNR

*Author to whom correspondence should be addressed. E-mail address: dwh@phys.tsinghua.edu.cn

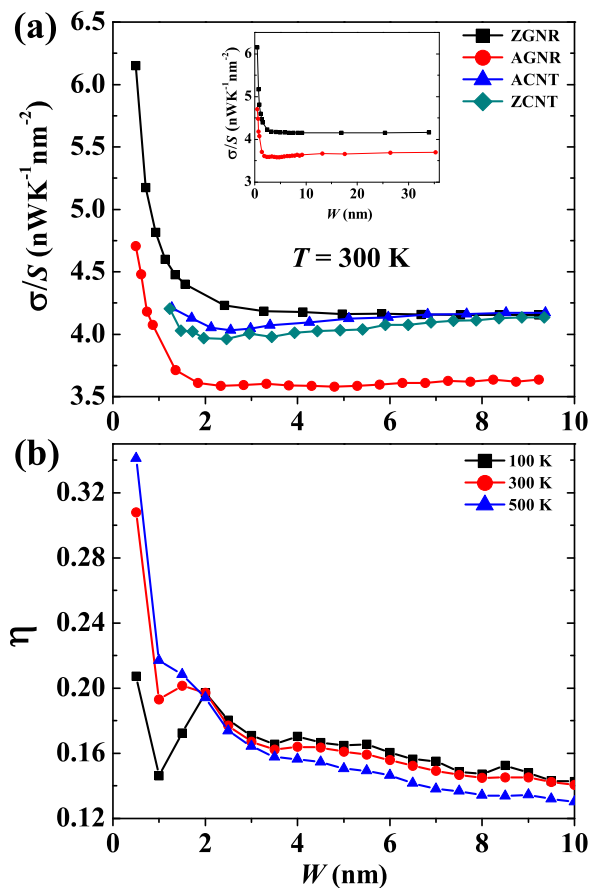


FIG. 2: (Color online) (a) The scaled thermal conductance (σ/S) at 300 K versus width (W) for ZGNRs (black square), AGNRs (red circle), ACNTs (blue triangle) and ZCNTs (cyan diamond). The inset shows σ/S for ZGNRs and AGNRs with the width varying from 0.5 to 35 nm. (b) The anisotropy factor (η) versus width (W) at 100 K (black square), 300 K (red circle) and 500 K (blue triangle). The lines are drawn to guide the eyes.

(N_z -ZGNR) denotes an AGNR (a ZGNR) with N_a (N_z) carbon dimer lines (zigzag carbon chains) across the ribbon width, as shown in Fig. 1. For the sake of comparison, armchair carbon nanotubes (ACNTs) and zigzag carbon nanotubes (ZCNTs) are also considered and their widths refer to their circumferences.

Fig. 2(a) shows the scaled thermal conductance (σ/S) at 300 K versus width for GNRs. It is interesting to see that GNRs exhibit different properties with respect to carbon nanotubes (CNTs). ACNTs have nearly the same scaled thermal conductance as ZCNTs, consistent with previous theoretical results¹¹. Moreover, the scaled thermal conductance of CNTs changes only slightly as the width changes. In one word, the scaled thermal conductance of CNTs is almost independent of their chirality and size. This, however, is not the case in GNRs, where significant size effect and anisotropy of thermal conductance are observed. For GNRs narrower than 2 nm, the scaled thermal conductance decreases rapidly as the width increases; while for wider GNRs, it changes very

slowly. More important, ZGNRs have significantly larger scaled thermal conductance than AGNRs, indicating a strong anisotropic thermal transport in GNRs. For example, when the width is larger than 2 nm, the scaled thermal conductance of ZGNRs at 300 K is around 4.2 nW/K/nm^2 , which is close to that of CNTs, while that of AGNRs is about 3.6 nW/K/nm^2 . The room temperature thermal conductance per unit area of wide GNRs is of the same order as that of pristine SiNWs ($\sim 1 \text{ nW/K/nm}^2$)⁶. However, graphene has much larger room temperature thermal conductivity ($\sim 5 \times 10^4 \text{ W/K/m}$)¹⁹ than SiNWs ($\sim 6 \text{ W/K/m}$ for a 22 nm diameter SiNW)²⁰, because the phonon mean free path is much longer in graphene than in SiNWs.

To give a quantitative description of the anisotropic thermal conductance, we further define an anisotropy factor for the thermal conductance as $\eta = [(\sigma/S)_{\text{ZGNR}}/(\sigma/S)_{\text{AGNR}}] - 1$. Fig. 2(b) shows the anisotropy factor η of GNRs with the width ranging from 0.5 to 10 nm at different temperatures (100, 300 and 500 K). It can be seen that narrower GNRs generally exhibit stronger anisotropy. However, the variation of the anisotropy factor is irregular at all temperatures when W is less than 2 nm. At 300 K, the anisotropy factor changes irregularly from 31% to 20% when the width varies from 0.5 nm to 2 nm, and decrease monotonously to 14% as the width increases to 10 nm. When the temperature changes from 100 K to 500 K, the anisotropy factor changes little except for very narrow GNRs. Moreover, the anisotropy factor will decrease rapidly when the temperature decreases from 100 K (the data is not shown here).

One can expect the anisotropy factor of GNRs will decrease to zero when the width is large enough, since thermal conductance is isotropic in graphene sheets.²¹ It is important to determine the critical width at which the anisotropy of thermal conductance disappears. We have extended our calculations to the ribbon width up to 35 nm. As shown in the inset of Fig. 2(a), the scaled thermal conductance varies very slowly with the width for wide GNRs. The anisotropy factor of 35 nm wide GNR still has a value of 13% at 300 K. Obviously, a direct calculation of thermal conductance at critical width using the NEGF method is beyond our computational capability. So we apply linear regression to fit the data from 4 to 35 nm for ZGNRs and AGNRs, and find that the anisotropy may disappear when $W \sim 140$ nm at 300 K.

What is the origin of anisotropic thermal conductance in GNRs? It was once attributed to different phonon scattering rates at the edges.⁹ For ideal structures without defects, however, there will be no boundary scattering at all, since the boundary structure is incorporated into the phonon modes. In fact, our results show the anisotropy still exists even without edge scattering. It was previously revealed that the anisotropic thermal conductance of SiNWs can be reproduced from the anisotropic phonon structure of bulk silicon⁶. Differently, graphene, the bulk counterpart of GNRs, is isotropic in thermal conductance. This suggests that for GNRs, boundary condition at edges instead of the bulk property is the origin of anisotropy.

The effect of the boundary condition on thermal conductance is rather complicated. Since lattice vibration is a collec-

tive behavior, almost every phonon modes will change if the boundary condition varies. Moreover, thermal conductance is always contributed by many phonon modes, and thus the total effect can not be demonstrated by focusing on particular phonon modes, but should be analyzed from the whole transmission. Fig. 3(a) shows the phonon transmission function for 16-ZGNR and 28-AGNR, which have a similar width ($W \sim 3.3$ nm). Only negligible difference in transmission is observed at low frequency region ($\omega < 100$ cm^{-1}), implying that the anisotropy disappears when the temperature is lower than 25 K. This indicates that the boundary condition has little influence on low frequency phonon modes. In contrast, obvious effect of boundary condition can be seen at high frequency region (especially at $400 \sim 600$ cm^{-1} and $1400 \sim 1650$ cm^{-1}): the transmission of 28-AGNR is always lower than that of 16-ZGNR. In principle, transmission function of ballistic transport is determined by the number and the dispersion of phonon bands. More dispersive phonon bands would give larger transmission. Since the two GNRs have nearly the same number of atoms per unit volume, the discrepancy should not be caused by different number of phonon bands. Comparing with zigzag edge, armchair edge indeed gives more localized lattice vibrations and less dispersive phonon bands, resulting in the anisotropic thermal conductance in GNRs.

The dependence of the scaled thermal conductance on temperature is illustrated in Fig. 3(b) for 16-ZGNR and 28-AGNR. As expected, the conductance increases monotonously with increasing temperature. Evidently, 16-ZGNR always has larger scaled thermal conductance than 28-AGNR. The anisotropy factor is small at low temperatures and keeps around 16% from 100 K to 500 K (data is not shown). Since the scaled thermal conductance only slightly varies with the width when the width is larger than 2 nm, it can be used to determine the maximum phonon thermal conductance at different temperatures for wide GNRs. Thermal conductance of a ZGNR (an AGNR) ($W > 2$ nm) can be estimated through multiplying the scaled thermal conductance of 16-ZGNR (28-AGNR) by the cross sectional area.

To further understand the effect of boundary condition on anisotropic thermal conductance, we artificially impose fixed boundary condition on the above two GNRs (i.e., 16-ZGNR and 28-AGNR) by setting the mass of edge atoms to 1.0×10^7 atomic mass unit in the calculation. Fixing edge atoms causes a decrease of scaled thermal conductance for both GNRs, as shown in Fig. 3(b). The scaled thermal conductance of 16-ZGNR decreases noticeably, especially at high temperatures, whereas the decrease of 28-AGNR is relatively small. After imposing fixed boundary condition the anisotropy becomes smaller but does not disappear. This shows the anisotropy is robust even in this extreme condition, which is substantially different from the free or periodic boundary condition generally used.

It should be noted that both phonon and electron transport can contribute to thermal conductance in practice. The electronic thermal conductance of gated GNRs was well discussed in Ref. 22. Since recent experiments showed that all sub-10-nm GNRs are semiconducting,²³ thermal conductance in GNRs narrower than 10 nm should be mostly dominated by

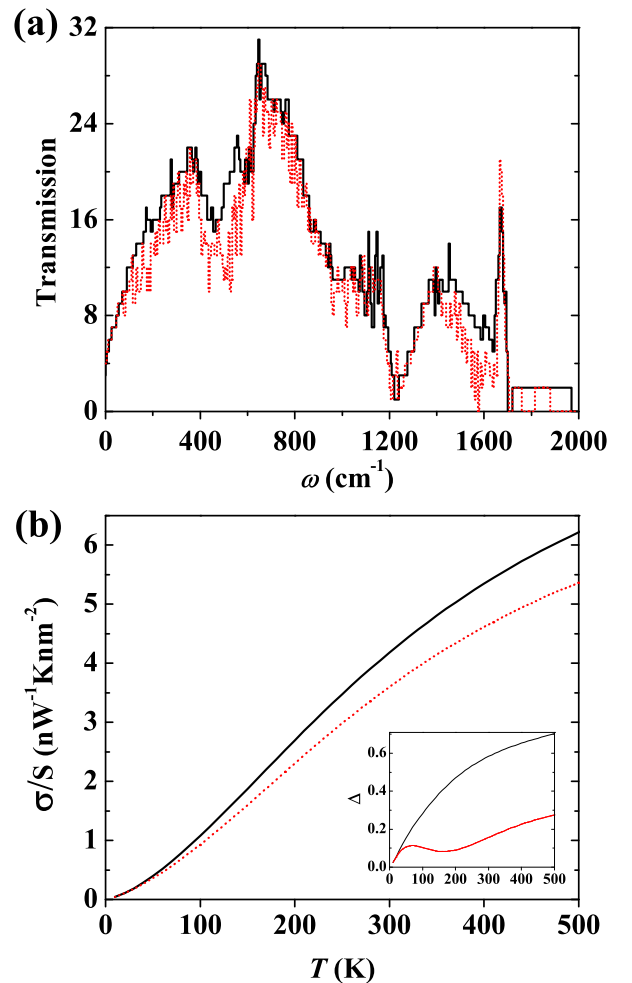


FIG. 3: (Color online) (a) Transmission function versus phonon frequency (ω) and (b) the scaled thermal conductance (σ/S) versus temperature (T) for 16-ZGNR (black solid line) and 28-AGNR (red dotted line). The inset shows the decrease of scaled thermal conductance (Δ) induced by fixing edge atoms.

phonons at all temperatures. While for GNRs of several tens of nm wide, the contribution from electrons might become important at low temperatures.

In conclusion, we have systematically studied thermal conductance for ZGNRs and AGNRs with the ribbon width ranging from 0.5 to 35 nm. Similar to electronic property, thermal conductance can also be tuned by the ribbon width and edge shape. The scaled thermal conductance (σ/S) decreases as the width increases and becomes nearly width independent when width is larger than 2 nm. More interestingly, ZGNRs have 13% \sim 31% larger thermal conductance than AGNRs at 300 K, showing that thermal conductance is anisotropic in GNRs. Unlike in SiNWs, the anisotropy in GNRs is caused by different boundary condition at edge but not the bulk phonon structure. Comparing with zigzag edge, armchair edge gives flatter phonon bands and behaves more like a fixed boundary. The intrinsic anisotropy found here is not limited to GNRs, but is also expected to appear in other materials with hexag-

onal structure, and is strong enough to be observable experimentally. Our work provides useful insight into the thermal management in GNR-based nanoelectronic and thermoelectric devices.

- ¹ A. H. Castro Neto, F. Guinea, N. M. R. Peres, K. S. Novoselov, and A. K. Geim, *Rev. Mod. Phys.* **81**, 109 (2009); and references therein.
- ² Y. W. Son, M. L. Cohen, and S. G. Louie, *Nature* **444**, 347 (2006).
- ³ Q. Yan, B. Huang, J. Yu, F. Zheng, J. Zang, J. Wu, B.-L. Gu, F. Liu, and W. Duan, *Nano Lett.* **7**, 1469 (2007).
- ⁴ Z. Li, H. Qian, J. Wu, B.-L. Gu, and W. Duan, *Phys. Rev. Lett.* **100**, 206802 (2008).
- ⁵ E. Pop, S. Sinha, and K. E. Goodson, *Proc. IEEE* **94**, 1587 (2006).
- ⁶ T. Markussen, A.-P. Jauho, and M. Brandbyge, *Nano Lett.* **8**, 3771 (2008).
- ⁷ T. Yamamoto and K. Watanabe, *Phys. Rev. B* **70**, 245402 (2004).
- ⁸ J. Lan, J.-S. Wang, C. K. Gan, and S. K. Chin, *Phys. Rev. B* **79**, 115401 (2009).
- ⁹ J. Hu, X. Ruan, and Y. P. Chen, *Nano Lett.* **9**, 2730 (2009).
- ¹⁰ The thermal conductivity given by Ref. 9 is about 2000 W/m/K at 400 K for a 5.7 nm long, 1.5 nm wide ZGNR, and the related thermal conductance is about 176 nW/K, much larger than the maximum thermal conductance (about 3 nW/K) from our ballistic phonon transport calculations. It was previously pointed out that molecular dynamics simulation is inadequate to describe quantum ballistic transport and can lead to the substantial violation of the ballistic upper bounds to thermal conductance (see Ref. 11).
- ¹¹ N. Mingo and D. A. Broido, *Phys. Rev. Lett.* **95**, 096105 (2005).
- ¹² T. Yamamoto and K. Watanabe, *Phys. Rev. Lett.* **96**, 255503 (2006).
- ¹³ N. Mingo, *Phys. Rev. B* **74**, 125402 (2006).
- ¹⁴ Y. Xu, J.-S. Wang, W. Duan, B.-L. Gu, and B. Li, *Phys. Rev. B* **78**, 224303 (2008).
- ¹⁵ J.-S. Wang, J. Wang, and J. T. Lü, *Eur. Phys. J. B* **62**, 381 (2008).
- ¹⁶ S. Ghosh, I. Calizo, D. Teweldebrhan, E. P. Pokatilov, D. L. Nika, A. A. Balandin, W. Bao, F. Miao, and C. N. Lau, *Appl. Phys. Lett.* **92**, 151911 (2008).
- ¹⁷ D. W. Brenner, O. A. Shenderova, J. A. Harrison, S. J. Stuart, B. Ni, and S. B. Sinnott, *J. Phys.: Condens. Matter* **14**, 783 (2002).
- ¹⁸ M. Vandescoren, P. Hermet, V. Meunier, L. Henrard, and Ph. Lambin, *Phys. Rev. B* **78**, 195401 (2008).
- ¹⁹ A. A. Balandin, S. Ghosh, W. Bao, I. Calizo, D. Teweldebrhan, F. Miao, and C. N. Lau, *Nano Lett.* **8**, 902 (2008).
- ²⁰ D. Li, Y. Wu, P. Kim, L. Shi, P. Yang, and A. Majumdar, *Appl. Phys. Lett.* **83**, 2934 (2003).
- ²¹ K. Saito, J. Nakamura, and A. Natori, *Phys. Rev. B* **76**, 115409 (2007).
- ²² E. Watanabe, S. Yamaguchi, J. Nakamura, and A. Natori, *Phys. Rev. B* **80**, 085404 (2009).
- ²³ X. Li, X. Wang, L. Zhang, S. Lee, and H. Dai, *Science* **319**, 1229 (2008).

This work was supported by the Ministry of Science and Technology of China (Grant No. 2006CB605105 and 2006CB0L0601), the National Natural Science Foundation of China.